Russian Journal of Earth Sciences Online ISSN: 1681-1208

Statistics of Wave Heights, Crests, and Troughs During the Black Sea Storm in November 2023

A. V. Garmashov[1], **and A. S. Zapevalov**[1,*]

[1]Marine Hydrophysical Institute, Russian Academy of Sciences, Sevastopol, Russian Federation
* **Correspondence to:** Alexander Zapevalov, sevzepter@mail.ru

Abstract: The changes in the characteristics of freak waves during an extreme storm in the Black Sea in November 2023 were analyzed based on direct measurement data from a stationary oceanographic platform located off the southern coast of Crimea. The height of individual waves reached up to 7.2 m, with a maximum significant height of 3.7 m. The continuous three-day wave record was divided into 20-min fragments, for which statistical characteristics of the waves were calculated. Three types of abnormality indices were analyzed based on the excess of wave height, crest height, and trough depth over a given level. During the storm, all abnormality indices increased, indicating that the probability of freak wave occurrences was higher than under ordinary conditions. When the significant wave height exceeded 2 m, it was often observed that the trough depth was greater than the crest height.

Keywords: extreme storm, freak waves, crest, trough, abnormality index, excess kurtosis, Black Sea

Citation: Garmashov A. V. and Zapevalov A. S. (2026), Statistics of Wave Heights, Crests, and Troughs During the Black Sea Storm in November 2023, *Russian Journal of Earth Sciences*, 26, ES3019, EDN: DASTNL, https://doi.org/10.2205/2026es001107

Review

Received: July 2, 2025
Accepted: March 2, 2026
Published: September 18, 2026

1. Introduction

In November 2023, an extreme storm formed in the Black Sea, which led to significant destruction of embankments, piers, and coastal structures of Crimea. The wave height in the central part of the sea exceeded 8 m, and the maximum wave periods exceeded 13 s [*Dulov et al.*, 2024]. The return period of storms with the characteristics of the Black Sea storm in November 2023 is 25 years [*Goryachkin et al.*, 2025]. To study extreme Black Sea storms, wave data, numerical modeling of wave fields, and remote sensing data from spacecraft were used [*Divinsky and Kosyan*, 2018; *Divinsky and Saprykina*, 2024; *Goryachkin and Repetin*, 2009; *Myslenkov et al.*, 2023].

Studies of extremely large storm waves are of great interest for coastal protection and maritime traffic [*Bernardino et al.*, 2020]. Waves of extremely large size, also called freak, rogue, or giant waves, are responsible for the loss of many ships and many human lives [*Kharif and Pelinovsky*, 2003]. The physical mechanism behind the occurrence of freak waves is not yet fully understood [*Kharif et al.*, 2009]. This is apparently due to the fact that freak waves arise as a result of several physical mechanisms, such as modulation instability (Benjamin-Feir instability) of wave packets [*Dyachenko and Zakharov*, 2005; *Dyachenko et al.*, 2013; *Zakharov and Ostrovsky*, 2009], nonlinear self-focusing [*Forristall*, 2005], interaction of waves with the current, geometric focusing, and nonlinear interaction of non-parallel wave systems [*Gerber*, 1993; *Hjelmervik and Trulsen*, 2009]. Currently, the prevailing opinion is that the appearance of anomalous waves is associated with the nonlinearity of the wave field [*Zakharov et al.*, 2006].

The presence of freak waves is usually characterized by the abnormality index AI_H [*Glejin et al.*, 2014; *Guedes Soares et al.*, 2003]:

$$AI_H = \frac{H_{\max}}{H_S},$$

where H is the wave height, and H_S is the significant wave height. Freak waves are those whose height is more than twice the significant height of background waves, i.e., waves for which the condition is met:

$$AI_H > 2. \quad (1)$$

Along with condition (1), another condition is used to identify freak waves [*Cattrell et al.*, 2018; *Zapevalov and Garmashov*, 2022]:

$$AI_{Cr} = \frac{Cr}{H_S} > 1.25, \quad (2)$$

where Cr is the height of the crest.

It has been noted in a number of works that in field conditions there are situations when the depth of the trough is greater than the height of the crest [*Didenkulova and Anderson*, 2010; *Glejin et al.*, 2014; *Zapevalov*, 2024]. Such situations are not described within the framework of the second-order nonlinear theory [*Zapevalov*, 2025]. It seems appropriate, by analogy with Equation (2), to introduce and analyze another parameter associated with the appearance of anomalous waves:

$$AI_{Th} = \frac{Th}{H_S},$$

where Th is the depth of the trough. We will select the condition $AI_{Th} > 1.25$ as the criterion for identifying freak waves. The introduction of this parameter is of great interest for solving engineering problems associated with the design of offshore drilling rigs [*Toffoli et al.*, 2008].

The aim of this study is to analyze the changes in the statistics of wave heights, crests, and troughs in the coastal area of the Black Sea during the extreme storm that occurred in November 2023. The analysis uses wave measurement data from the oceanographic platform of the Marine Hydrophysical Institute of the Russian Academy of Sciences, which is located off the southern coast of Crimea.

2. Statistical Description

The procedure for isolating an individual wave is described in detail in [*Forristall*, 2000; *Stansell et al.*, 2003]. On a wave record, an individual wave is defined as a part of it between any two consecutive zero down-crossings or up-crossings. In this work, individual waves were determined as part of the zero down-crossing procedure. The main parameters characterizing the individual wave are the crest height, the trough depth, and the wave height. The crest height Cr is the maximum vertical distance from mean sea level to the maximum of the crest. The trough depth Th is the vertical distance from the mean sea level to the trough minimum, and it is always positive. The wave height here is defined as the sum of the trough depth and the crest height that follows it: $H = Th + Cr$.

It was shown earlier that the type of distribution of the crest height and trough depth depends significantly on the nonlinearity of sea waves [*Zapevalov and Garmashov*, 2024]. Cumulants of surface elevations $\eta(t)$ of the third and fourth order (skewness λ_3 and excess kurtosis λ_4) are usually used as parameters characterizing the level of nonlinearity of the wave field [*Janssen*, 2003; *Luxmoore et al.*, 2019; *Wang et al.*, 2022]. Cumulants are defined as:

$$\lambda_3 = \frac{m_3}{m_2^{3/2}}, \quad \lambda_4 = \frac{m_4}{m_2^2} - 3,$$

where $m_n = \langle \eta^n \rangle$ is the statistical moment about the mean of order n, and the angle brackets denote averaging.

The parameters characterizing the energy of the wave field are the variance of surface elevations m_2 or significant height H_S. These parameters are related through the equation $H_S = 4\sqrt{m_2}$.

3. Wave Measurements

During the storm, direct wave measurements were carried out at a stationary oceanographic platform located in the Black Sea off the southern coast of Crimea. The platform is located 600 m from the shore, at a depth of 28 m. The analysis uses data from continuous wave measurements taken between November 25 and 27, 2023. Wave measurements were carried out with a sampling interval of 0.25 s. A string wave recorder was used for the measurements [*Garmashov*, 2019]. Simultaneously with the wave measurements, meteorological parameters were measured. The maximum wind speed during the storm, reduced to a height of 10 m, was 37 m/s.

The elevation measurements of the sea surface were carried out using a resistive wave recorder. The wave recorder sensor is made of nichrome wire with a diameter of 0.5 mm, which is wound with a standardized pitch on the carrier cable. The sensor is connected to a unit that converts its active resistance into a normalized analog output signal.

The wave recorder does not have a nonlinear relationship between the signal level and the sea surface elevation; this was, in particular, verified before placement by step-by-step (1 m) measurement of the sensor resistance. According to the device's specifications, wave height is measured in the 0–10 m range with a resolution of 0.03 m and a sampling rate of 4 Hz. The measurement error is $(0.03 + 0.01H)$ m, where H is the measured wave height.

The increase in error with increasing wave height is mainly due to the measurement technique that is inherent in most wave recorders of this type. The vertical orientation of the wave recorder sensor is provided by a massive weight placed as close as possible to the bottom. This structure is not rigidly fixed to the bottom and may be subject to slight tilts due to the influence of sea currents. The sensor tilt in the wave records is visible as a change in the average sea level. During the storm of November 25–27, 2023, no significant changes in the average sea level were observed in the wave records.

During the storm period, long-period waves were recorded, which is unusual for the Black Sea [*Dulov et al.*, 2024]. The minimum value of the ratio between the water depth at the platform location and the dominant wavelength was 0.154, which leads to a deviation from the linear dispersion relation. This effect does not affect the calculations of the crest heights and trough depths.

All data passed quality control, and individual outliers were removed. For each wave record, a frequency spectrum was obtained, which was calculated using the classical method as the Fourier transform of the correlation function. Tukey windows were used for smoothing, and the number of degrees of freedom varied from 21 to 77. The spectrum was used to monitor the presence or absence of high-frequency noise in the measured signal. The analysis showed that there were no high-frequency noise during the measurement period. The frequency of dominant waves ω_0 was also determined from the spectrum. Signal variations with frequencies below $0.5\omega_0$ were excluded.

4. Abnormality Index

The continuous wave record was divided into fragments, 20 min long. Wave statistics were calculated for each fragment. Changes in the main parameters characterizing the state of the sea surface during a storm are shown in Figure 1. The subscript "max" shows that this parameter is the maximum for a 20-min fragment. The value T_0 corresponds to the time 00:00 on November 25, 2023. The vertical lines show the moments of time when the significant wave height exceeded the level of 2 m (T_1), and when it dropped below 2 m (T_2). The time interval $T_2 - T_1$ is 10 h.

It is noteworthy that in the region where $H_S > 2$ m, the maximum depth of the trough in most cases exceeds the maximum height of the crest. Outside the specified region, the opposite relationship is observed, $Cr_{\max > Th_{\max}}$. The effect of the trough depth exceeding the crest height has been previously observed in various experiments conducted by different researchers [*Didenkulova and Anderson*, 2010; *Glejin et al.*, 2014; *Zapevalov*, 2024]. It is not described within the framework of a second-order nonlinear theory, just as the emergence

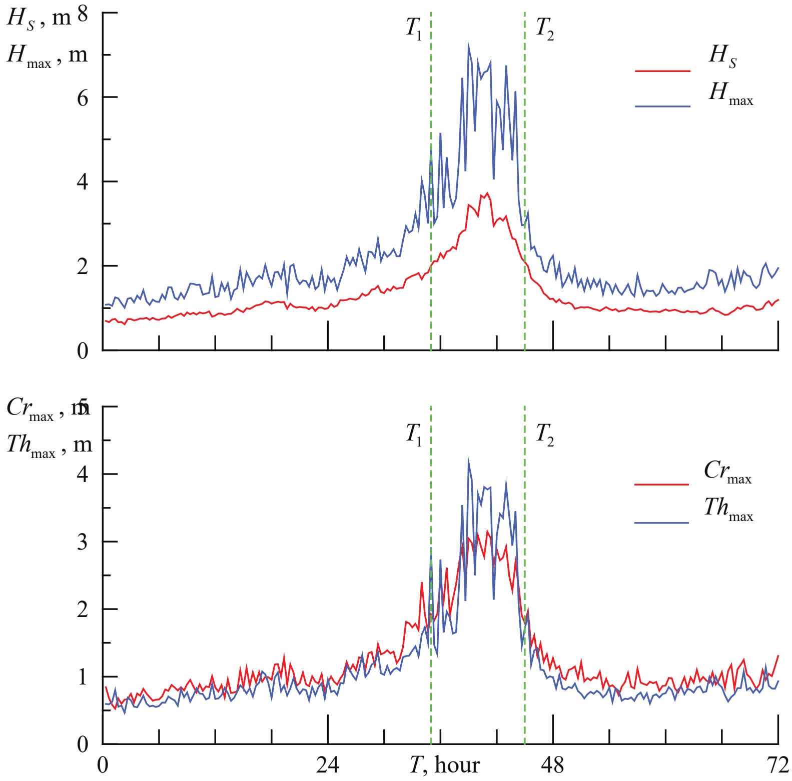

Figure 1. Wave statistics during the storm of November 25–27, 2023. The upper fragment describes changes in the significant H_S and maximum H_{max} wave heights. The lower fragment describes changes in the maximum crest heights Cr_{max} and trough depths Th_{max}.

of a negative skewness in the distribution of sea surface elevations, which was observed in many experiments [*Zapevalov*, 2025], is not described.

The distributions of crest heights and trough depths are usually analyzed within the framework of a model constructed on the basis of the expansion of the wave profile into a series in powers of a small parameter. In the narrow-band spectrum approximation, a simplified second-order nonlinear model is proposed to describe the statistical characteristics, which is the sum of two components [*Tayfun*, 1980]. The model is described by the equation of the amplitude-modulated Stokes wave:

$$\eta(x,t) = a_r(x,t)\cos(k_p x - \omega t + \varepsilon) + \frac{1}{2}k_p a_r^2(x,t)\cos(2(k_p x - \omega t + \varepsilon)), \quad (3)$$

where $a_r(x,t)$ is the wave envelope, k_p is the wave number corresponding to the peak of the wave spectrum, ω is the average frequency, and ε is the random phase. The local maxima of the second term in Equation (3) coincide with the crest and trough of the linear wave described by the first term. The height of the crest and the depth of the trough within this model are respectively equal [*Toffoli et al.*, 2008]:

$$Cr = a_r + \frac{1}{2}k_p a_r^2, \quad Th = a_r - \frac{1}{2}k_p a_r^2,$$

therefore, the inequality $Cr > Th$ holds.

Here, model (3) is presented with the aim of clearly showing in a simple analytical form that, within the framework of a second-order nonlinear model, the height of the crest is always greater than the depth of the trough. In all currently existing nonlinear models, the condition $Cr > Th$ is satisfied, and the skewness of the surface elevations is always positive [*Zapevalov*, 2025].

Changes in the abnormality indices are shown in Figure 2. Here, horizontal lines show the levels, exceeding which allows us to consider the wave as a freak wave. It is evident that during a storm, the probability of the occurrence of anomalous waves corresponding to condition (1) increases. The indices AI_{Cr} and AI_{Th} in the time domain between T_1 and T_2 also increase. The probability of the occurrence of anomalous waves according to criterion (1) is higher than according to criterion (2). This is due to the existence of freak waves in which the trough depth is greater than the crest height [*Zapevalov and Garmashov*, 2024].

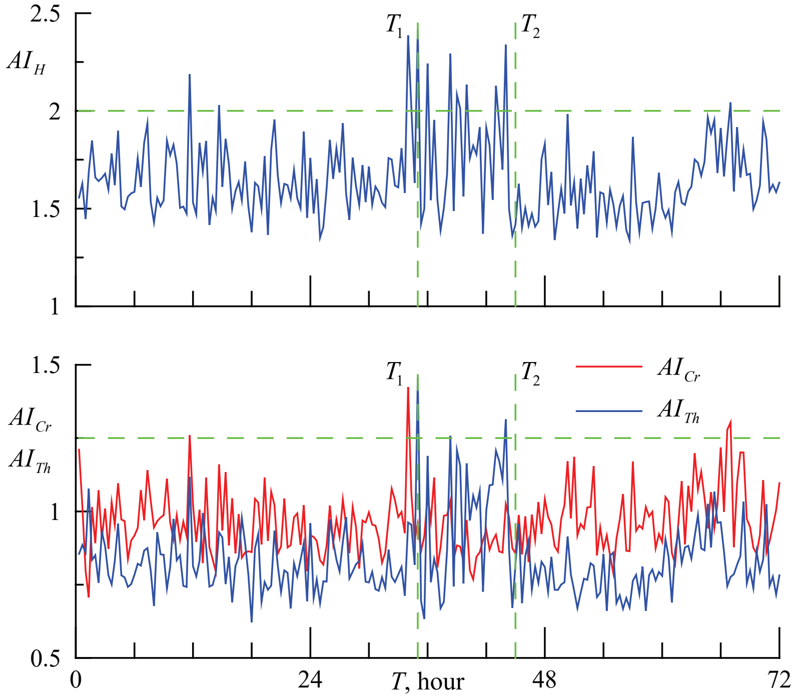

Figure 2. Changes in the abnormality indices AI_H, AI_{Cr}, and AI_{Th} during the storm.

It should be noted that there is no statistical relationship between the abnormality indices AI_{Cr} and AI_{Th}. For the data shown in Figure 2, the correlation coefficient $R(AI_{Th}, AI_{Cr}) = 0.08$.

Previous studies have shown that the only wave parameter for which there is a statistical dependence on AI_H is excess kurtosis [*Guedes Soares et al.*, 2003; *Shin and Hong*, 2009; *Wang et al.*, 2015; *Zapevalov and Garmashov*, 2022]. The data obtained during the storm confirmed the existence of such a relationship. The correlation coefficient between AI_H and λ_4, calculated for the entire array of data shown in Figure 3, is equal to $R(AI_H, \lambda_4) = 0.65$. If only data in the time domain from T_1 to T_2 are used to calculate the correlation coefficient, then $R(AI_H, \lambda_4) = 0.77$. The linear regression equation relating AI_H and λ_4 is of the form:

$$AI_H = 0.39\lambda_4 + 1.58.$$

The abnormality indices AI_{Cr} and AI_{Th} also depend on the excess kurtosis. The correlation coefficients had the following values: $R(AI_{Cr}, \lambda_4) = 0.45$ and $R(AI_{Th}, \lambda_4) = 0.58$.

5. Methodological Features of Calculating Wave Heights

Two methods are used to calculate the parameters of individual waves; these methods are zero down-crossings and zero up-crossings. In the first method, the wave height is defined as the sum of the crest and the trough that precedes it; in the second method, height is defined as the sum of the crest and the trough that follows it. Two troughs may differ, and therefore the wave heights will also differ. Let us compare the heights of freak

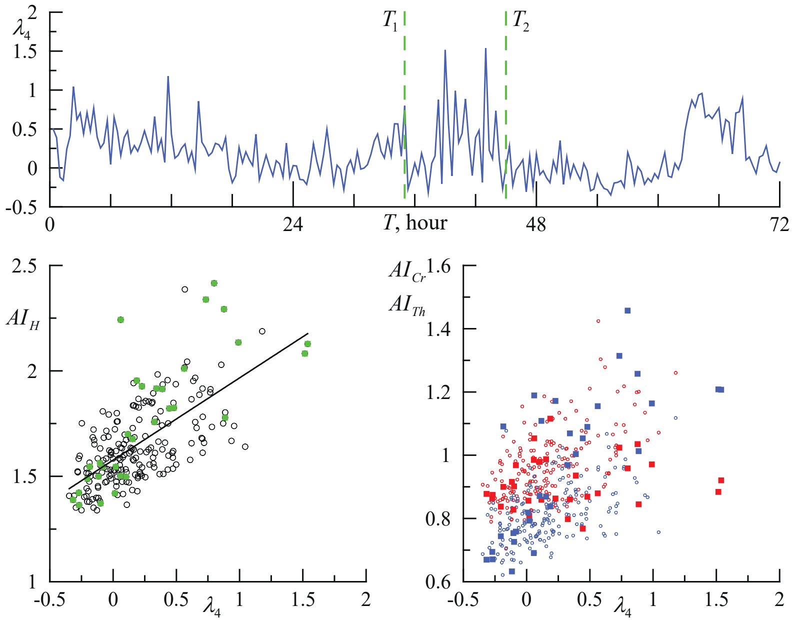

Figure 3. Dependences of the abnormality indices AI_H (black), AI_{Cr} (red), and AI_{Th} (blue) on the excess kurtosis λ_4. The squares highlight the values obtained in the time domain from T_1 to T_2. Linear regression is shown by the lines of the corresponding color.

waves determined by these two methods in the time period $T_1 \leq t \leq T_2$. Figure 4 shows, as an example, fragments of a wave record 100 s long, each of which contains one freak wave.

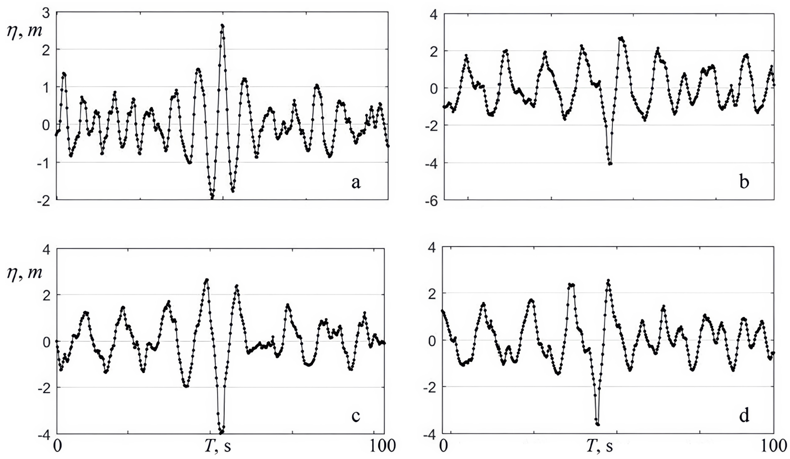

Figure 4. Fragments of wave records including freak waves.

In the analyzed data array, situations are observed in which the trough Th_d preceding the crest of the freak wave is larger than the trough Th_u following its crest, as well as situations in which $Th_d < Th_u$. The heights of the freak waves determined by different methods vary significantly. Situations in which $Th_d > Th_u$ accounted for approximately 80 %.

There are several types of anomalous waves. The first type includes waves in which the crest is larger than the trough (fragment a). The second type comprises waves in which the trough is larger than the crest (fragments b, c, and d). Situations where the trough is larger than the crest were observed in approximately 70 % of cases.

A small number of freak waves recorded during a single storm does not allow obtaining reliable estimates of the recurrence frequency of situations where freak waves satisfy the condition $Th_d > Th_u$ or $Th > Cr$. These studies need to be continued using larger datasets.

6. Conclusions

The wave measurement data obtained during the extreme storm in the Black Sea in November 2023 allowed us to estimate the probability of freak waves at different stages of its development.

To identify freak waves, three types of criteria were used based on exceeding the wave height, crest height, and trough depth of a given level (abnormality indices AI_H, AI_{Cr}, and AI_{Th}). It is shown that all abnormality indices are statistically related to the excess kurtosis of sea surface elevations. The likelihood of freak waves occurring during a storm is higher than before it starts and after it ends.

When the significant height was greater than 2 m, situations were often observed in which the maximum (for 20 min) trough depth was greater than the maximum crest height. This effect cannot be described within the framework of second-order nonlinear theory. Further research is needed to understand the physical causes of this phenomenon.

Funding. This work was completed within the framework of the state assignment on the topic FNNN-2024-0014 “Fundamental studies of interaction processes in the sea-air system that form the physical state variability of the marine environment at various spatial and temporal scales”.

References

Bernardino M., Rusu L. and Guedes Soares C. Evaluation of extreme storm waves in the Black Sea // Journal of Operational Oceanography. — 2020. — Vol. 14, no. 2. — P. 114–128. — https://doi.org/10.1080/1755876x.2020.1736748

Cattrell A. D., Srokosz M., Moat B. I., et al. Can rogue waves be predicted using characteristic wave parameters? // Journal of Geophysical Research: Oceans. — 2018. — Vol. 123, no. 8. — P. 5624–5636. — https://doi.org/10.1029/2018jc013958

Didenkulova I. and Anderson C. Freak waves of different types in the coastal zone of the Baltic Sea // Natural Hazards and Earth System Sciences. — 2010. — Vol. 10, no. 9. — P. 2021–2029. — https://doi.org/10.5194/nhess-10-2021-2010

Divinsky B. V. and Kosyan R. D. Wave climate of the coastal zone of the Crimean peninsula // Physical Oceanography. — 2018. — Vol. 25, no. 2. — P. 93–101. — https://doi.org/10.22449/1573-160x-2018-2-93-101

Divinsky B. V. and Saprykina Ya. V. Extreme wind waves on the northeastern shelf of the Black Sea // Doklady Earth Sciences. — 2024. — Vol. 517, no. 1. — P. 1224–1233. — https://doi.org/10.1134/s1028334x24601676

Dulov V. A., Yurovskaya M. V., Fomin V. V., et al. Extreme Black Sea Storm in November, 2023 // Physical Oceanography. — 2024. — Vol. 31, no. 2. — P. 295–316.

Dyachenko A. I. and Zakharov V. E. Modulation instability of Stokes wave → freak wave // Journal of Experimental and Theoretical Physics Letters. — 2005. — Vol. 81, no. 6. — P. 255–259. — https://doi.org/10.1134/1.1931010

Dyachenko A. I., Zakharov V. E., Shamin R. V., et al. Rogue waves and tasks of their study // The World Ocean. Vol. 1. Geology and tectonics of the Ocean. Catastrophic phenomena in the Ocean / ed. by L. I. Lobkovsky. — Scientific World Publ., 2013. — P. 576–592. — (In Russian).

Forristall G. Z. Wave Crest Distributions: Observations and Second-Order Theory // Journal of Physical Oceanography. — 2000. — Vol. 30, no. 8. — P. 1931–1943. — https://doi.org/10.1175/1520-0485(2000)030<1931:wcdoas>2.0.co;2

Forristall G. Z. Understanding rogue waves: Are new physics really necessary? // Rogue Waves: Proc. 14th ’Aha Huliko’a Hawaiian Winter Workshop. — Honolulu, USA, 2005.

Garmashov A. Hydrometeorological monitoring on the stationary oceanographic platform in the Black Sea // 19th International Multidisciplinary Scientific GeoConference SGEM2019, Water Resources. Forest, Marine and Ocean Ecosystems. Vol. 19. — STEF92 Technology, 2019. — P. 259–264. — https://doi.org/10.5593/sgem2019/3.1/s12.034

Gerber M. The interaction of deep-water gravity waves and an annular current: linear theory // Journal of Fluid Mechanics. — 1993. — Vol. 248. — P. 153–172. — https://doi.org/10.1017/s0022112093000722

Glejin J., Sanil Kumar V., Nair T. M. B., et al. Freak waves off Ratnagiri, west coast of India // Indian Journal of Geo-Marine Sciences. — 2014. — Vol. 43, no. 7. — P. 1339–1342.

Goryachkin Yu. N., Markov A. A. and Fomin V. V. Impacts of the November 26–27, 2023 storm on the coast of Crimea // Hydrotechnika. — 2025. — No. 1. — P. 32–40. — (In Russian).

Goryachkin Yu. N. and Repetin L. N. Storm wind-wave regime off the Black Sea coast of Crimea // Ecological Safety of Coastal and Shelf Zones and comprehensive use of shelf resources. — Sevastopol, 2009. — Vol. 19. — P. 56–69. — (In Russian).

Guedes Soares C., Cherneva Z. and Antão E. M. Characteristics of abnormal waves in North Sea storm sea states // Applied Ocean Research. — 2003. — Vol. 25, no. 6. — P. 337–344. — https://doi.org/10.1016/j.apor.2004.02.005

Hjelmervik K. and Trulsen K. Freak wave statistics on collinear currents // Journal of Fluid Mechanics. — 2009. — Vol. 637. — P. 267–284. — https://doi.org/10.1017/s0022112009990607

Janssen P. A. E. M. Nonlinear Four-Wave Interactions and Freak Waves // Journal of Physical Oceanography. — 2003. — Vol. 33, no. 4. — P. 863–884. — https://doi.org/10.1175/1520-0485(2003)33<863:nfiafw>2.0.co;2

Kharif C. and Pelinovsky E. Physical mechanisms of the rogue wave phenomenon // European Journal of Mechanics - B/Fluids. — 2003. — Vol. 22, no. 6. — P. 603–634. — https://doi.org/10.1016/j.euromechflu.2003.09.002

Kharif C., Pelinovsky E. and Slunyaev A. Rogue waves in the ocean. — Springer Berlin Heidelberg, 2009. — 216 p. — https://doi.org/10.1007/978-3-540-88419-4

Luxmoore J. F., Ilic S. and Mori N. On kurtosis and extreme waves in crossing directional seas: a laboratory experiment // Journal of Fluid Mechanics. — 2019. — Vol. 876. — P. 792–817. — https://doi.org/10.1017/jfm.2019.575

Myslenkov S., Kruglova E., Medvedeva A., et al. Number of Storms in Several Russian Seas: Trends and Connection to Large-Scale Atmospheric Indices // Russian Journal of Earth Sciences. — 2023. — Vol. 23. — ES3002. — https://doi.org/10.2205/2023es000828

Shin S.-H. and Hong K. Nonlinear Parameters of Wave Distribution to Characterize Freak Waves // Rogue Waves 2008 : Proceedings of a Workshop organized by Ifremer and held in Brest, France 13-14-15 October 2008 within the Brest Sea Tech Week 2008. — Brest, France : ifremer, 2009. — P. 157–158.

Stansell P., Wolfram J. and Zachary S. Horizontal asymmetry and steepness distributions for wind-driven ocean waves from severe storms // Applied Ocean Research. — 2003. — Vol. 25, no. 3. — P. 137–155. — https://doi.org/10.1016/j.apor.2003.10.001

Tayfun M. A. Narrow-band nonlinear sea waves // Journal of Geophysical Research: Oceans. — 1980. — Vol. 85, no. C3. — P. 1548–1552. — https://doi.org/10.1029/jc085ic03p01548

Toffoli A., Bitner-Gregersen E., Onorato M., et al. Wave crest and trough distributions in a broad-banded directional wave field // Ocean Engineering. — 2008. — Vol. 35, no. 17/18. — P. 1784–1792. — https://doi.org/10.1016/j.oceaneng.2008.08.010

Wang L., Li J. and Li S. Numerical Simulation of Freak Wave Generation in Irregular Wave Train // Journal of Applied Mathematics and Physics. — 2015. — Vol. 03, no. 08. — P. 1044–1050. — https://doi.org/10.4236/jamp.2015.38129

Wang L., Zhou B., Jin P., et al. Relation between occurrence probability of freak waves and kurtosis/skewness in unidirectional wave trains under single-peak spectra // Ocean Engineering. — 2022. — Vol. 248. — P. 110813. — https://doi.org/10.1016/j.oceaneng.2022.110813

Zakharov V. E., Dyachenko A. I. and Prokofiev A. O. Freak waves as nonlinear stage of Stokes wave modulation instability // European Journal of Mechanics - B/Fluids. — 2006. — Vol. 25, no. 5. — P. 677–692. — https://doi.org/10.1016/j.euromechflu.2006.03.004

Zakharov V. E. and Ostrovsky L. A. Modulation instability: The beginning // Physica D: Nonlinear Phenomena. — 2009. — Vol. 238, no. 5. — P. 540–548. — https://doi.org/10.1016/j.physd.2008.12.002

Zapevalov A. S. Statistical distributions of crests and trough of sea surface waves // Ecological Safety of Coastal and Shelf Zones of Sea. — 2024. — No. 3. — P. 49–58. — (In Russian).

Zapevalov A. S. Global View on Statistical Models of Sea Surface Elevations // Russian Journal of Earth Sciences. — 2025. — Vol. 25. — ES1006. — https://doi.org/10.2205/2025es000952

Zapevalov A. S. and Garmashov A. V. Probability of the Appearance of Abnormal Waves in the Coastal Zone of the Black Sea at the Southern coast of Crimea // Ecological Safety of Coastal and Shelf Zones of Sea. — 2022. — No. 3. — P. 6–15. — https://doi.org/10.22449/2413-5577-2022-3-6-15 — (In Russian).

Zapevalov A. S. and Garmashov A. V. Ratio between trough and crest of surface waves in the coastal zone of the Black Sea // Physical Oceanography. — 2024. — Vol. 31, no. 1. — P. 71–78.